

---

EFDA–JET–CP(01)02-08

P. Dumortier, P. Andrew, G. Bonheure, R.V. Budny, R. Buttery, M. Charlet, I. Coffey, M. de Baar, P.C. de Vries, T. Eich, D. Hillis, C. Ingesson, C. Liu, G. Maddison, S.Jachmich, G. Jackson, A. Kallenbach, H.R. Koslowski, K.D. Lawson, A.M. Messiaen, P. Monier-Garbet, M. Murakami, M.F.F. Nave, J. Ongena, V. Parail, M.E. Puiatti, J. Rapp, F.Sartori, M. Stamp, J. Strachan, W. Suttrop, G. Telesca, M. Tokar, B. Unterberg, M. Valisa, M. von Hellermann, B. Weyssow and JET EFDA Contributors

# Confinement Properties of High Density Impurity Seeded ELMy H-Mode Discharges at Low and High Triangulaity on JET



# Confinement Properties of High Density Impurity Seeded ELMy H-Mode Discharges at Low and High Triangulaity on JET

P. Dumortier<sup>1</sup>, P. Andrew<sup>2</sup>, G. Bonheure<sup>1</sup>, R.V. Budny<sup>3</sup>, R. Buttery<sup>2</sup>, M. Charlet<sup>2</sup>, I. Coffey<sup>2</sup>,  
M. de Baar<sup>4</sup>, P.C. de Vries<sup>4</sup>, T. Eich<sup>5</sup>, D. Hillis<sup>6</sup>, C. Ingesson<sup>4</sup>, C. Liu<sup>7</sup>, G. Maddison<sup>2</sup>,  
S.Jachmich<sup>1</sup>, G. Jackson<sup>8</sup>, A. Kallenbach<sup>9</sup>, H.R. Koslowski<sup>5</sup>, K.D. Lawson<sup>2</sup>,  
A.M. Messiaen<sup>1</sup>, P. Monier-Garbet<sup>10</sup>, M. Murakami<sup>8</sup>, M.F.F. Nave<sup>11</sup>, J. Ongena<sup>1</sup>, V. Parail<sup>2</sup>,  
M.E. Puiatti<sup>12</sup>, J. Rapp<sup>5</sup>, F.Sartori<sup>2</sup>, M. Stamp<sup>2</sup>, J. Strachan<sup>3</sup>, W. Suttrop<sup>9</sup>, G. Telesca<sup>12</sup>,  
M. Tokar<sup>5</sup>, B. Unterberg<sup>5</sup>, M. Valisa<sup>12</sup>, M. von Hellermann<sup>4</sup>, B. Weysow<sup>7</sup>  
and JET EFDA Contributors\*

<sup>1</sup>LPP-ERM/KMS, "Euratom-Belgian State" Association, Brussels, Belgium<sup>†</sup>

<sup>2</sup>EURATOM/UKAEA Fusion Association, Culham Science Center, Abingdon, UK

<sup>3</sup>Princeton Plasma Physics Laboratory, Princeton, USA

<sup>4</sup>FOM-Rijnhuizen, Association Euratom-FOM, PO Box 1207, 3430 BE Nieuwegein, NL<sup>†</sup>

<sup>5</sup>Institut für Plasmaphysik, Euratom Association, Forschungszentrum Jülich GmbH, Germany<sup>†</sup>

<sup>6</sup>ORNL, Oak Ridge, USA

<sup>7</sup>ULB, "Euratom-Belgian State" Association, Brussels, Belgium

<sup>8</sup>DIII-D National Fusion Facility, San Diego, USA

<sup>9</sup>Max-Planck Insitut für Plasmaphysik, Euratom Association, Garching, Germany

<sup>10</sup>Association Euratom-CEA, DRFC, CEA Cadarache, St Paul lez Durance, France

<sup>11</sup>Associação Euratom-IST, Centro de Fusão Nuclear, Lisbon, Portugal

<sup>12</sup>Associazione Euratom-ENEA sulla Fusione, Consorzio RFX, Padova, Italy

<sup>†</sup>Partners in the Trilateral Euregio Cluster (TEC)

\*See appendix of the paper by J.Pamela "Overview of recent JET results",  
Proceedings of the IAEA conference on Fusion Energy, Sorrento 2000

Preprint of Paper to be submitted for publication in Proceedings of the  
EPS Conference,  
(Maderia, Portugal 18-22 June 2001)

“This document is intended for publication in the open literature. It is made available on the understanding that it may not be further circulated and extracts or references may not be published prior to publication of the original when applicable, or without the consent of the Publications Officer, EFDA, Culham Science Centre, Abingdon, Oxon, OX14 3DB, UK.”

“Enquiries about Copyright and reproduction should be addressed to the Publications Officer, EFDA, Culham Science Centre, Abingdon, Oxon, OX14 3DB, UK.”

## ABSTRACT

The ITER-FEAT reference operational scenario for pulsed operation at  $Q = 10$  is ELMy H-mode with a confinement characterized by  $H_{98}(y,2) = 1$  at  $f_{GW} = n/n_{GW} = 0.85$ , where  $H_{98}(y,2)$  is the enhancement factor over the IPB98(y,2) scaling law [1] and  $f_{GW}$  is the Greenwald factor i.e. the density normalized to the empirical Greenwald density limit  $n_{GW}$  [2]. Previous experiments on JET and other tokamaks [3] have shown that the energy confinement degrades when raising density towards  $n_{GW}$  and that the maximum achievable density for a given confinement is increasing with the triangularity  $\delta$ . Hence the necessity to develop scenarios combining high confinement at high density. However, high confinement is generally accompanied by large type I ELMs of low frequency causing severe transient power loads on the divertor target plates. The power load may be reduced by radiating a substantial part of the energy over greater surface areas. This can be achieved by the seeding of impurities into the plasma, trying to create a radiating mantle. These experiments aim at combining high density, high confinement and good power exhaust by a radiating plasma edge without altering significantly the purity of the plasma center.

### 1. SEPTUM EXPERIMENTS

A first series of experiments was carried out in the septum configuration, i.e. with the X-point lying on the dome of the MkIIIGB divertor (fig.1). This configuration was chosen because it was the divertor configuration the closest to the pumped limiter configuration of TEXTOR where the promising RI-mode, combining all the requested attractive features, was developed [4]. Whereas no H-mode like transitions occurs during the TEXTOR RI-mode, this configuration is characterized by a low L-H power threshold allowing to keep the H-mode while radiating a large fraction of the power. Operational conditions are:  $I_p = 2.5\text{MA}$ ,  $B_t = 2.4\text{T}$ ,  $q_{95} \approx 3.05$ ,  $P_{NBI} = 11 \rightarrow 15\text{MW}$ ,  $P_{ICRH} = 0 \rightarrow 3\text{MW}$ .

### 2. SEPTUM LOW TRIANGULARITY DISCHARGES ( $\kappa = 1.65$ , $\delta_1 = 0.24$ , $\delta_u = 0.18$ )

High fuelling rates are used to rise the density in these discharges but lead to strong confinement degradation. After the switch-off of the gas injection (“afterpuff” phase) the confinement recovers to H-mode quality whereas the density stays near the value reached at the end of the main fuelling phase (fig.2, boxes 1, 2, 3). In fig.2, the blue traces correspond to an unseeded reference discharge whereas the red and green traces correspond to discharges where Ar was seeded respectively in the puff phase - main fuelling phase - only and in both the puff and afterpuff phases (fig. 2, box 4). The seeding of Ar in the initial main fuelling phase allows to rise the density even closer to the Greenwald value (fig.2, box 2), but at the expense of a further confinement degradation (fig.2, box 1) accompanied by a change of the ELM character from type I to type III. Small levels of  $D_2$  are puffed in the afterpuff phase in order to counteract the density decay without degrading the recovered confinement. Small amounts of Ar need to be seeded in order to keep the radiation level (fig. 2, box 5) and also helps to keep the density.

Finally, by careful tailoring of the refueling of Ar and  $D_2$  in the “afterpuff” phase (green traces) we could obtain a discharge where the ITER-FEAT requested density and confinement were simultaneously

obtained and maintained up to the technical limit for the heating, i.e. for about 12 energy confinement times. The radiated power fraction in the afterpuff rises from 35% for the unseeded case up to 45% in the seeded case, the radiation increase coming mainly from inside the separatrix in the septum region [6]. It is worthwhile to note that the value of  $Z_{\text{eff}}$  measured by visible Bremsstrahlung is also maintained constant around 2 and is even lower than in the unseeded reference case due to the higher density reached. Moreover, the ELM behavior is modified in presence of Ar: ELMs are slower and the ELM losses seem to be reduced [5]. Another favorable feature is that the density profile may peak (fig.3) without rise in  $Z_{\text{eff}}$ . This scheme is very sensitive to the good dosing of the maintenance puffs ( $D_2$  and Ar) in the afterpuff. Indeed, higher levels of Ar lead to dramatic confinement loss correlated with sawteeth suppression, possibly ELM-free phases, impurity accumulation leading to higher radiation of the impurities from the center [6] and enhanced MHD activity [7]. The impurity accumulation could be avoided and hence the stationarity of the discharges improved by keeping adequate sawtooth activity by heating of the center using ICRH in order to keep  $q_0 < 1$  [8].

### 3. SEPTUM HIGH TRIANGULARITY DISCHARGES ( $\kappa = 1.73$ , $\delta_1 = 0.29$ , $\delta_u = 0.33$ )

A few discharges were performed at a higher triangularity on the septum and although the fuelling of the discharges wasn't optimized for stationarity, the effects described above remain qualitatively the same except that in this latter case, higher densities are reached at the end of the puff phase without Ar seeding and the seeding of Ar doesn't this time allow to increase further the achieved densities. A scan of the plasma position didn't show any clear influence of the proximity of the walls and the better fuelling efficiency is attributed to the higher  $\delta$ .

### 4. EXTREMELY HIGH TRIANGULARITY EXPERIMENTS

Small amounts of Ar were also seeded in high  $\delta$  discharges ( $\delta_u \approx 0.5$ ) with large heating power (with respect to the L-H power threshold) and large  $D_2$  fuelling. The X-point is here well above the septum (fig.4). These plasmas (with  $I_p = 2.3\text{MA}$ ,  $B_t = 2.4\text{T}$ ,  $q_{95} \approx 3.05$ ,  $P_{\text{NBI}} \approx 14\text{ MW}$ ,  $P_{\text{ICRH}} \approx 2\text{MW}$ ) show exceptional performances as displayed in fig. 5 (red traces): normalized density  $f_{\text{GW}} \approx 1$  as well as  $H98(y,2) \approx 1$  [8]. In this case, the seeding of Ar (fig.5, green traces) leads to a continuous rise of the density to even higher values.  $Z_{\text{eff}}$  is slightly higher ( $\Delta Z_{\text{eff}} = 0.2$ ) and there's a slight confinement penalty with  $H98(y,2)$  nevertheless remaining close to unity. The major difference resides in the higher total radiated power fraction (going from 45% to 65%), the increase in radiation coming mainly from the edge [6]. Moreover, measurements with the IR camera show dramatic reduction of the divertor target temperature in the Ar seeded case. However dedicated experiments have to be carried out to clearly assess the potential effect of mitigation of the ELMs by impurity seeding. In the example of fig.5, the brutal reduction of  $D_2$  fuelling at 22s leads to an increased effect of the seeded Ar leading to enhanced central radiation: the density further increases, the beam power is less and less centrally deposited and the small amount of ICRH is insufficient to avoid the collapse of the central electron temperature.

## CONCLUSIONS

This work has shown it was possible to achieve simultaneously the ITER-FEAT requested conditions for density ( $n/n_{GW} \geq 0.85$ ) and confinement ( $H_{98}(y,2) \approx 1$ ) with good indications of reduced ELM losses due to the presence of seeded impurities. The major results were obtained in two different configurations. The first one is the septum configuration where the adequate conditions could be sustained in the afterpuff phase up to the technical limit ( $\approx 12$  energy confinement times) in the low  $\delta$  case. Higher  $\delta$  as well as seeding of Ar allows to reach higher densities in the puff phase. Confinement drops in the puff phase due to large  $D_2$  fuelling and is recovered in the afterpuff phase where the density can be maintained by careful fuelling of  $D_2$  and Ar. Impurity accumulation and stationarity of the discharges can be improved by central ICRH in order to keep the sawtooth activity. The second configuration is a high  $\delta$  one with large fuelling and heating power. The seeding of Ar allows essentially to radiate a larger part of the power (65% instead of 45%), mainly from the edge, at the expense of slightly higher  $Z_{eff}$  ( $\Delta Z_{eff} = 0.2$ ) and moderate confinement penalty. It also allows reaching higher densities. This scenario needs further investigation in order to clearly assess the effect of impurity seeding on ELM mitigation and to have a better control of the density and of the stationarity of the discharge (by acting on the fuelling levels and on the central heating).

## ACKNOWLEDGEMENTS

This work has been conducted under the European Fusion Development Agreement

## REFERENCES

- [1]. ITER Physics Basis, Nucl. Fusion **39** (1999) 2208
- [2]. Greenwald, M., et al., Nucl. Fusion **28** (1988) 2199
- [3]. Saibene, G., et al., Nucl. Fusion **39** (1999) 1133
- [4]. Weynants, R.R., et al., Nucl. Fusion **39** (1999) 1637
- [5]. Jachmich, S., et al., this conference
- [6]. Puiatti, M.E., et al., this conference
- [7]. Koslowski, H.R., et al., this conference
- [8]. Nave, M.F., et al., this conference
- [9]. Saibene, G., et al., this conference

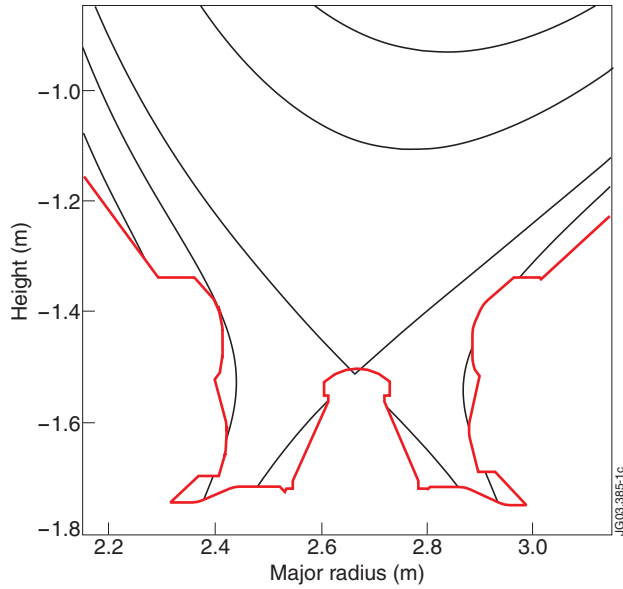


Figure 1: “Septum” configuration: the X-point is lying on the dome of the MkiIGB divertor

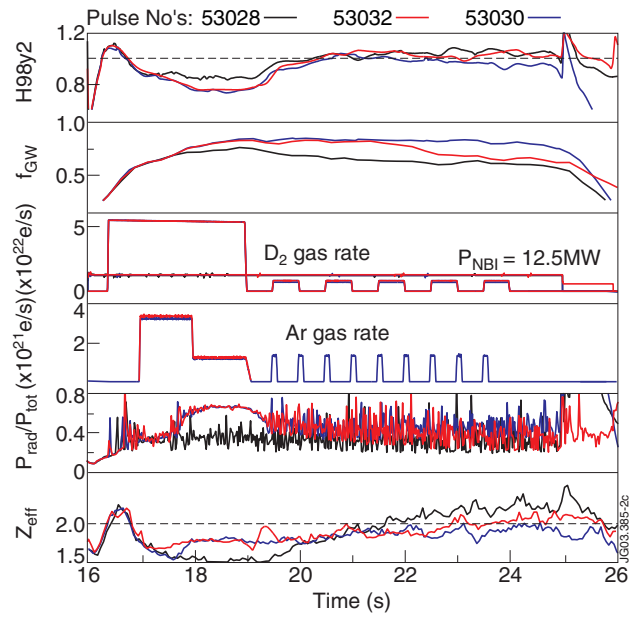


Figure 2: Time traces of global plasma parameters for three discharges: unseeded reference (blue), with impurity seeding in the “puff” (red) and with impurity seeding both in the “puff” and in the “afterpuff” (green): confinement enhancement factor, Greenwald fraction, beam power and  $D_2$  gas rate, Ar gas rate, total radiated power fraction and  $Z_{eff}$

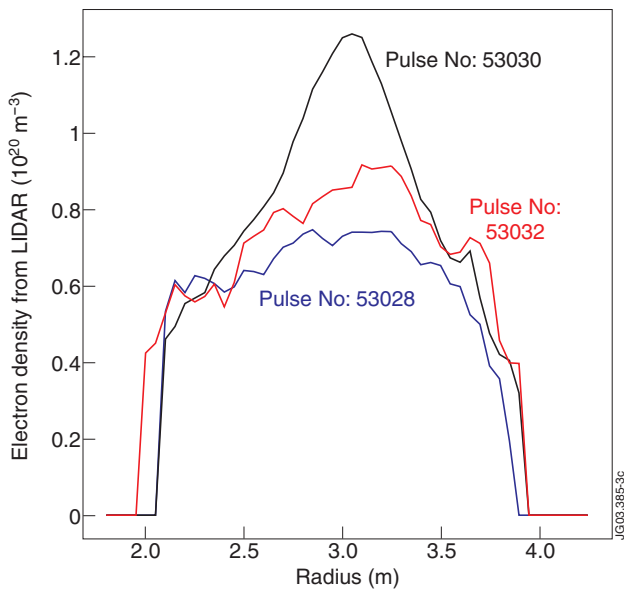


Figure 3: Density peaking for the three shots of fig.2 taken at 22.9s.

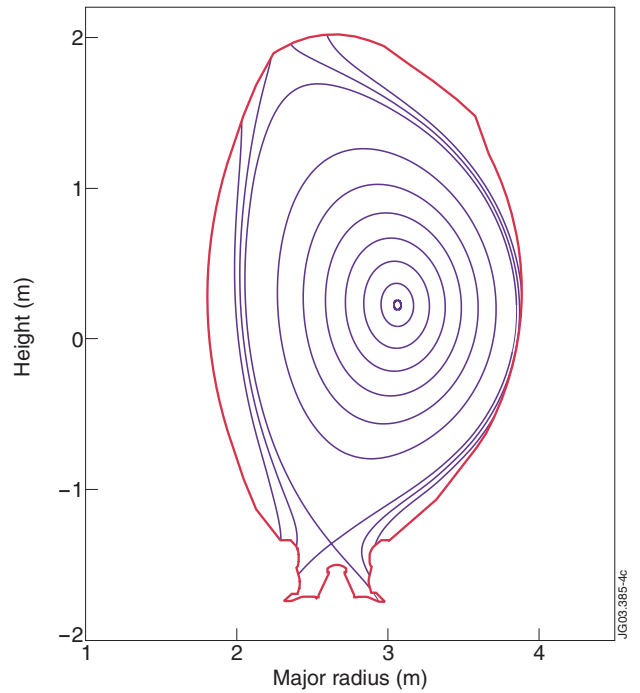


Figure 4: EHT magnetic configuration

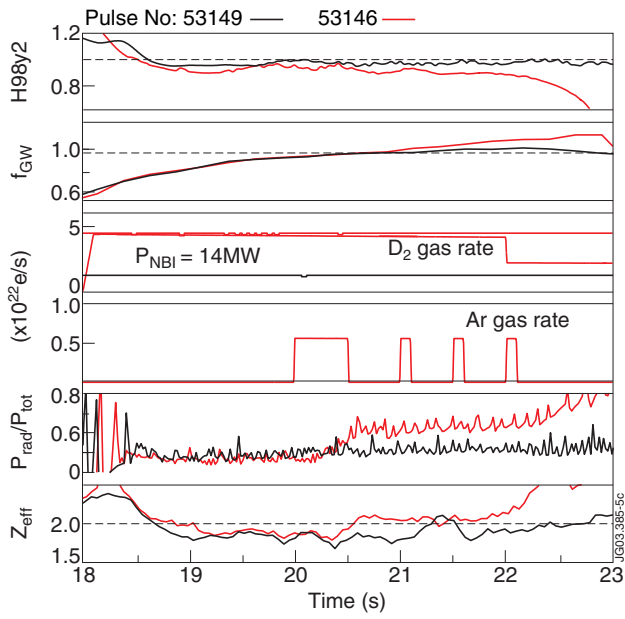


Figure 5: Time traces of global plasma parameters for two discharges: unseeded reference (red) and with impurity seeding (green): confinement enhancement factor, Greenwald fraction, beam power and  $D_2$  gas rate, Ar gas rate, total radiated power and  $Z_{eff}$ .